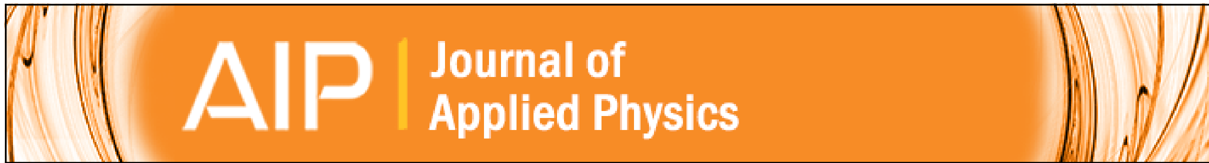

Modeling of high fluence Ti ion implantation and vacuum carburization in steel

D. Farkas, I. L. Singer, and M. Rangaswamy

Citation: Journal of Applied Physics **57**, 1114 (1985); doi: 10.1063/1.334554
View online: http://dx.doi.org/10.1063/1.334554
View Table of Contents: http://scitation.aip.org/content/aip/journal/jap/57/4?ver=pdfcov
Published by the AIP Publishing

Articles you may be interested in
Plasma source ion carburizing of steel for improved wear resistance
J. Vac. Sci. Technol. A **16**, 524 (1998); 10.1116/1.581071

High resistivity and picosecond carrier lifetime of GaAs implanted with MeV Ga ions at high fluences
Appl. Phys. Lett. **67**, 1724 (1995); 10.1063/1.115029

Durable metal carbide layers on steels formed by ion implantation at high temperatures
J. Appl. Phys. **58**, 1255 (1985); 10.1063/1.336117

Summary Abstract: Effects of pressure and temperature on implantation-induced carburization of steels
J. Vac. Sci. Technol. A **3**, 589 (1985); 10.1116/1.572956

Carburization of steel surfaces during implantation of Ti ions at high fluences
J. Vac. Sci. Technol. A **1**, 419 (1983); 10.1116/1.571934

MIT LINCOLN LABORATORY CAREERS
Discover the satisfaction of innovation and service to the nation
Space Control
Air & Missile Defense
Communications Systems & Cyber Security
Intelligence, Surveillance and Reconnaissance Systems
Advanced Electronics
Tactical Systems
Homeland Protection
Air Traffic Control

[This article is copyrighted as indicated in the article. Reuse of AIP content is subject to the terms at: http://scitation.aip.org/termsconditions. Downloaded to] IP: 128.173.126.47 On: Wed, 06 May 2015 20:53:19

Modeling of high fluence Ti ion implantation and vacuum carburization in steel

D. Farkas
Department of Materials Engineering, Virginia Polytechnic Institute and State University, Blacksburg, Virginia 24061.

I. L. Singer
Chemistry Division, Code 6170, Naval Research Laboratory, Washington, D.C. 20375.

M. Rangaswamy
Department of Materials Engineering, Virginia Polytechnic Institute and State University, Blacksburg, Virginia 24061.

(Received 22 March 1984; accepted for publication 30 July 1984)

Concentration-versus-depth profiles have been calculated for Ti and C in Ti-implanted 52100 steel. A computer formalism was developed to account for diffusion and mixing processes, as well as sputtering and lattice dilation. A Gaussian distribution of Ti was assumed to be incorporated at each time interval. The effects of sputtering and lattice dilation were then included by means of an appropriate coordinate transformation. C was assumed to be gettered from the vacuum system in a one-to-one ratio with the surface Ti concentration up to a saturation point. Both Ti and C were allowed to diffuse. A series of experimental (Auger) concentration-versus-depth profiles of Ti-implanted steel were analyzed using the above-mentioned assumptions. A best fit procedure for these curves yielded information on the values of the sputtering yield, range, and straggling, as well as the mixing processes that occur during the implantation. The effective diffusivity of Ti was found to be 6×10^{-15} cm^2/sec, a value that is consistent with the cascade mixing mechanism. The effective diffusivity of C was found to be 6×10^{-15} cm^2/sec, and the sputtering yield by Ti atoms was best fit by a value of about 2. The observed range and straggling values were in very good agreement with the values predicted by existing theories, so long as the lattice was allowed to dilate.

INTRODUCTION

Ions implanted to high fluences ($>10^{17}$ cm^2) in metals are capable of creating unique alloy surfaces with remarkable mechanical and chemical properties. An example of such an alloy is the wear-resistant amorphous layer formed when Ti is implanted into 52100 steel.[1] This layer forms by adsorbing carbon from residual gases in the vacuum chamber,[2] assisted by Ti atoms which reach the surface by sputter erosion during implantation.[3]

The mechanism by which carbon migrates into the solid (thermal diffusion, collision cascades, etc.) is not better understood today than at the time when the effect was first recognized. This is in part due to the lack of appreciation for vacuum/solid interactions but even more to the scarcity of models for high fluence implantation into solids.

The present paper describes a computational method for modeling high fluence implantation and presents calculated Ti and C depth profiles which mimic those observed for the above-mentioned Ti implantation into 52100 (Fe 1.5Cr-1C) steel. The model accounts for ion collection, sputtering, and lattice dilation in a manner similar to the earlier treatments by Schultz and Wittmaak[4] and Krautle.[5] It also considers the diffusion-like transport processes which affect the shape of the evolving profiles and incorporates the vacuum carburization process elucidated by Singer.[3] The computational method is based on a numerical solution of the coupled diffusion equations for implanted Ti and adsorbed C. Effective diffusivities for the two species and sputtering yield by Ti ions are obtained by comparison of the calculated and experimental profiles. The experimental data of the room temperature implantation modeled in the present work were obtained by Singer,[3] and are shown in Fig. 1. The Auger sputter depth profiles are believed to be accurate to $\pm$ 20% in both concentration and depth scales.

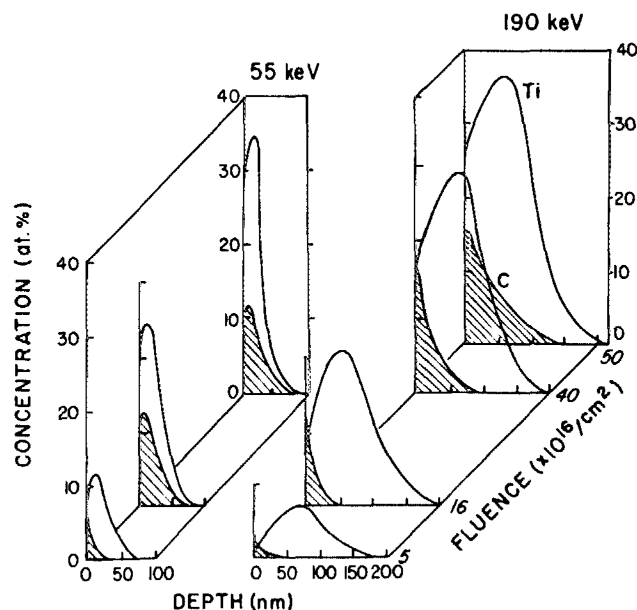

FIG. 1. Concentration-vs-depth profiles for Ti and C in Ti-implanted 52100 steel at several fluences and energies, obtained by Auger sputter profiling as described in Ref. 1. (Left) 5, 16, and 40×10^{16} Ti$^+$/cm^2 at 55 keV; (Right) 5, 16, 40, and 50×10^{16} Ti$^+$/cm^2 at 190 keV. Note: bulk C concentration of the steel (4 at. %) was subtracted from data.

[This article is copyrighted as indicated in the article. Reuse of AIP content is subject to the terms at: http://scitation.aip.org/termsconditions. Downloaded to] IP: 128.173.126.47 On: Wed, 06 May 2015 20:53:19

 © 1985 American Institute of Physics

THEORETICAL CONSIDERATIONS

The profile of Ti implanted to high fluences is affected by four processes:

(1) Ion collection, with a Gaussian distribution;

(2) sputter erosion of the surface;

(3) lattice dilation as a result of ion collection; and

(4) diffusion-like broadening resulting from the collision cascades or radiation-enhanced diffusion.

The adsorbed C profiles are affected by two processes:

(1) Surface buildup of C as a function of time; and

(2) diffusion-like penetration.

These processes and the way in which they are treated in the present formalism are described in detail in the following sections.

Diffusion-like processes

The term "diffusion-like" is used here to denote transport processes that obey Fick's second law[6]:

$$\frac{\partial[\mathrm{Ti}]}{\partial t} = D_{\mathrm{Ti}} \frac{\partial^2[\mathrm{Ti}]}{\partial x^2}, \tag{1a}$$

$$\frac{\partial[\mathrm{C}]}{\partial t} = D_{\mathrm{C}} \frac{\partial^2[\mathrm{C}]}{\partial x^2}, \tag{1b}$$

where [C] and [Ti] denote the concentrations of carbon and titanium, respectively, and D the effective diffusivity. These equations describe thermal and radiation-enhanced diffusion, as well as cascade mixing.[7]

Equations (1a) and (1b) were solved for D_{Ti} and D_{C} values which best fit all the experimental curves illustrated in Fig. 1. In these calculations D_{Ti} and D_{C} were approximated as constants, as suggested by the calculations of Eltoukhy *et al.*[8] Nonzero values for D_{Ti} indicate the relative importance of diffusion-like mixing under the conditions of implantation studied. We reemphasize that both D_{C} and D_{Ti} should be considered as effective diffusivities, since they may result from processes other than thermally activated diffusion.

The solution of Eqs. (1a) and (1b) requires the definition of boundary conditions. The ion collection process, as described below, was used as a boundary condition for Eq. (1a). For Eq. (1b) the boundary condition is the surface carbon concentration as a function of time, taken from the model for vacuum carburization presented by Singer.[3] Vacuum carburization can be understood in terms of a four-step process:

(1) Sputtering uncovers implanted Ti;

(2) surface Ti atoms adsorb carbonaceous molecules from residual gases in the vacuum chamber;

(3) surface carbide species are formed by dissociative chemisorption of molecules; and

(4) surface carbon atoms diffuse inwards.

The model predicts a surface concentration of C that is proportional to the amount of Ti exposed at the surface. As a first approximation it can be asumed that every exposed Ti atom adsorbs a C atom. This assumption is justified by the experimental data for surface contents up to concentrations around 16 at. % where there appears to be a saturation of the adsorbed carbon. Therefore, the boundary condition used in the solution of Eq. (1b) is that, at the surface, the C and Ti concentrations are equal.

The diffusion equations (1a) and (1b) were solved by a finite difference technique, the Cranck–Nicholson method.[6,9] The finite difference method, described in more detail in the appendix, is based on a space-time grid. The size of the space increment Δx was taken to be 1/30 of the total depth of penetration, and the size of the time increment Δt was taken as 1/50 of the total time of implantation for the particular fluence considered. The coupling between the two differential equations introduced by the boundary conditions required that the two equations be solved simultaneously. At each time step the profiles were adjusted as follows: A Gaussian distribution of collected Ti was added to the existing profile, which was initially zero; the C concentration at the surface was made equal to the Ti concentration; and the depth coordinates were transformed to account for the sputter erosion of the surface and the lattice dilation. The amount sputtered away δx during a time period Δt was calculated as

$$\delta x = (f S \Delta t)/n_0, \tag{2}$$

where f is the number of incoming ions per unit time, S is the sputtering yield, and n_0 is the atomic density of the implanted target.

Effect of lattice dilation

The method used to account for the effect of lattice dilation is similar to that used by Krautle.[5] The atomic density n_0 of the material was considered constant and the dilation of each space interval Δx was made proportional to the increment of implanted species collected in that space interval. This should be a good approximation for Ti implanted into Fe due to the similarity in their lattice parameters. In Krautle's calculations the total shift of a point x was computed analytically as the integral of the Gaussian distribution of the implanted species.

However, in our calculations, it was found more convenient to obtain the cumulative shift of a point x as a sum of the incremental dilations. This was done as follows: An increment Δx of index I was dilated during time Δt by an amount dx

$$dx(I) = \frac{\Delta x f \Delta t}{n_0} \frac{1}{\sqrt{\pi}\Delta R_p} \exp\left[-(I\Delta x - R_p)^2/(2\Delta R_p^2)\right], \tag{3}$$

where R_p and ΔR_p are the range and range straggling of the distribution. Thus after each implantation increment, coordinate x is transformed to x' as

$$x'(I) = x(I) + \epsilon(I) - \delta x, \tag{4}$$

where $\epsilon(I)$ is the cumulative dilation of increment I, given by

$$\epsilon(I) = \sum_{k=0}^{I} dx(k). \tag{5}$$

Equation (4) gives the coordinate transformation at each time increment for space interval I.

RESULTS

The formalism described requires the input of the following parameters

[This article is copyrighted as indicated in the article. Reuse of AIP content is subject to the terms at: http://scitation.aip.org/termsconditions. Downloaded to] IP: 128.173.126.47 On: Wed, 06 May 2015 20:53:19

TABLE I. Range and range straggling using LSS theory.

Energy	Most probable range R_p	Range straggling ΔR_p
55 keV	20 nm	8.6 nm
190 keV	59 nm	23 nm

(1) Range R_p and range straggling ΔR_p of Ti ions in steel: These values were obtained from calculations done using LSS theory as described in the Manning and Mueller procedure.[10] The values are shown in Table I.

(2) Flux of the incoming ions f which was obtained from the experimental conditions as fluence per unit time. The Ti flux was converted to added thickness per unit time, using the atomic density n_0 of the 52100 steel. ($f = 9.26 \times 10^{13}$ atoms/sec cm^2, $n_0 = 8.21 \times 10^{22}$ atoms/cm^3.)

(3) Effective diffusivity of C, which was varied in order to obtain a good fit with the experimental C profiles.

(4) Effective diffusivity of Ti which was varied in order to obtain the best fit to the experimental Ti profiles.

(5) Sputtering yield S: A value of the sputtering yield was obtained directly from the experimental data and indirectly by comparing computed curves using varying sputtering yields to the experimental profiles in a best fit procedure. A value of the sputtering yield was obtained directly from experimental data by considering the areas under the Ti profiles as a function of fluence and sputtering yield. The amount of Ti sputtered away is proportional to the surface concentration of Ti, the incoming flux and the sputtering yield. The retained dose of Ti, $A(t)$ is given by an integral over time of the incoming flux minus whatever was sputtered away.

$$A(t) = \int_0^t [f/n_0 - S(f/n_0)[\mathrm{Ti}]^s(t)]\, dt, \tag{6}$$

where $[\mathrm{Ti}]^s(t)$ is the surface concentration of Ti at time t. Schultz and Wittmaak calculated an expression for the surface concentration of an implanted species in the presence of sputtering, obtaining an expression in terms of error functions. In the present calculation the experimental data for the surface concentration was approximated by a linear function. This is a good approximation for low fluences.

$$[\mathrm{Ti}]^s(t) = kt, \tag{7}$$

where k is the slope of the surface concentration versus time curve and is obtained directly from experimental data. This has been shown to be a good approximation for the 190-keV case.[1] The sputtering yield can be calculated by substituting Eq. (7) into Eq. (6) and integrating. The analysis resulted in a value of $S = 1.9$ for Ti implantation in 52100 steel.

Lattice dilation was found to be very important. Calculations performed without lattice dilation required range and range straggling values that were very much different from the ones predicted by the Manning and Mueller formalism. For the 190-keV implant, the fitted values were $R_p = 90$ nm and $\Delta R_p = 50$ nm, which are almost double the LSS values shown in Table I. Since this discrepancy is unlikely, it was concluded that the lattice dilation effect is absolutely necessary to describe high fluence ion implantation profiles.

The next series of calculations included the lattice dilation effect but did not consider a diffusion-like process for Ti. The calculated curves were consistently narrower than the experimental ones, suggesting that a diffusion-like process was indeed necessary to account for the observed results. When both diffusion and lattice dilation were included in the calculations, only one combination of S and D_{Ti} values resulted in Ti profiles that fit all seven measured profiles. These values were $D_{\mathrm{Ti}} = 6 \times 10^{-15}$ cm^2/sec and $S = 2$.

The sensitivity of the profiles to the value of S can be seen in Fig. 2 for six of the seven experimental curves studied. (The profile for 190 keV at lowest fluence of 5×10^{16}/cm^2 was found to be insensitive to the variation of the parameters of interest and therefore is not shown.) Figure 2 shows

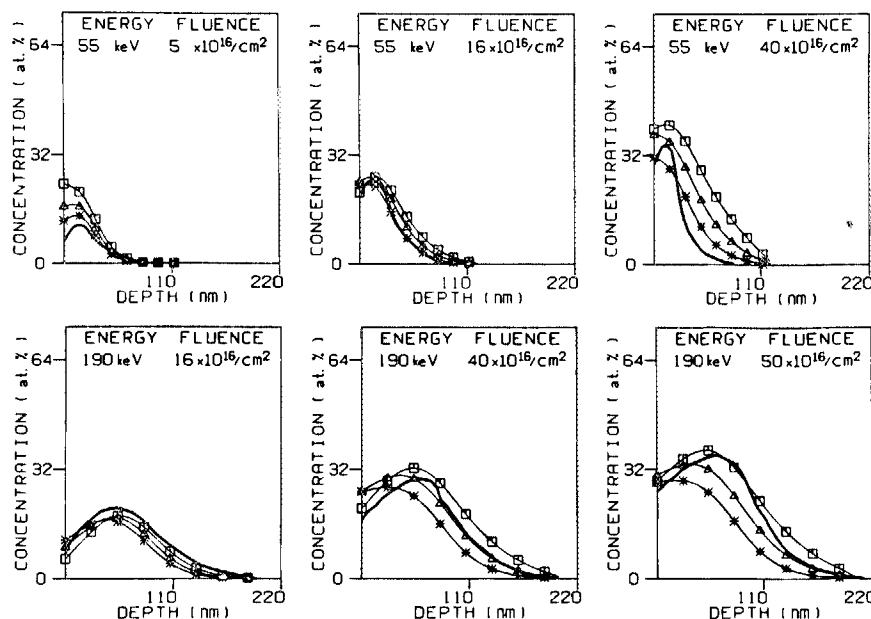

FIG. 2. Experimental (heavy line) and calculated Ti profiles for several values of S (□: 1.0; △: 2.0; ∗: 3.0), with $D_{\mathrm{Ti}} = 6 \times 10^{-15}$ (cm^2/s).

[This article is copyrighted as indicated in the article. Reuse of AIP content is subject to the terms at: http://scitation.aip.org/termsconditions. Downloaded to] IP: 128.173.126.47 On: Wed, 06 May 2015 20:53:19

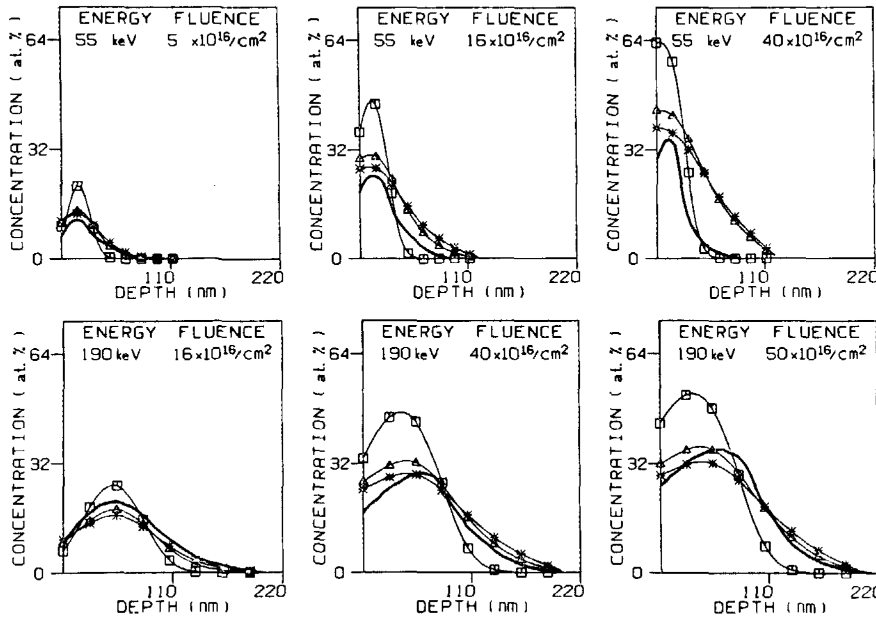

FIG. 3. Experimental (heavy line) and calculated Ti profiles for several values of $D_{\rm Ti}$ [□: 0; △: 6; *: 10($\times 10^{-15}$ cm^2/s)], with $S = 1.5$.

calculated and experimental Ti-versus-depth profiles for three fluences at each of two energies. As expected, the effect of increasing sputtering yield is to move the profiles closer to the surface. The value of S that best describes the experimental curves seems to decrease from a value somewhat greater than 2 to a value less than 2 as the fluence increases. This is consistent with the value of 1.9 derived directly from experimental data. The results of Fig. 2 were calculated for a Ti effective diffusivity of 6×10^{-15} cm^2/sec.

The sensitivity of the calculated profiles to the value of $D_{\rm Ti}$ is shown in Figs. 3 and 4. These figures show calculations done for sputtering yields of 1.5 and 2, respectively. These results include the ones obtained in the absence of diffusion broadening, showing that the experimental data are consistently broader. A value of $D_{\rm Ti}$ different from zero results in better agreement with experiment. An order of magnitude estimate of the transport process present can be obtained from these figures and it is approximately $D_{\rm Ti} = 6\times 10^{-15}$ cm^2/sec.

Figure 5 shows the calculated carbon concentration profiles compared to experiment. In this figure calculations are presented for different values of $D_{\rm C}$. For the lower fluences the value $D_{\rm C} = 6\times 10^{-15}$ cm^2/sec gives good agreement with the measured profiles. At higher fluences the agreement is not good because there appears to be a saturation of carbon at the surface. At high fluences the assumption used in the calculations that every Ti adsorbs a carbon is probably no longer valid. Figure 6 shows the results of calculations in which $[\rm C]^s$ is restricted to 16 at. %. The results are better than the ones without the saturation limit. It should also be noted that these calculations assume a sputtering yield of 2.0, which as discussed above seems to be too high

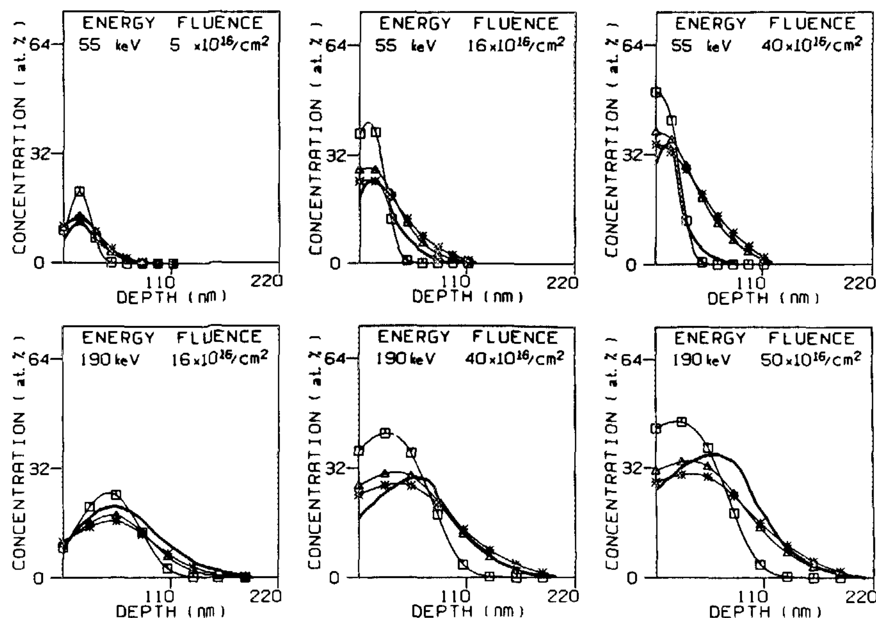

FIG. 4. Experimental (heavy line) and calculated Ti profiles for several values of $D_{\rm Ti}$ [□: 0; △: 6; *: 10($\times 10^{-15}$ cm^2/s)], with $S = 2$.

[This article is copyrighted as indicated in the article. Reuse of AIP content is subject to the terms at: http://scitation.aip.org/termsconditions. Downloaded to] IP: 128.173.126.47 On: Wed, 06 May 2015 20:53:19

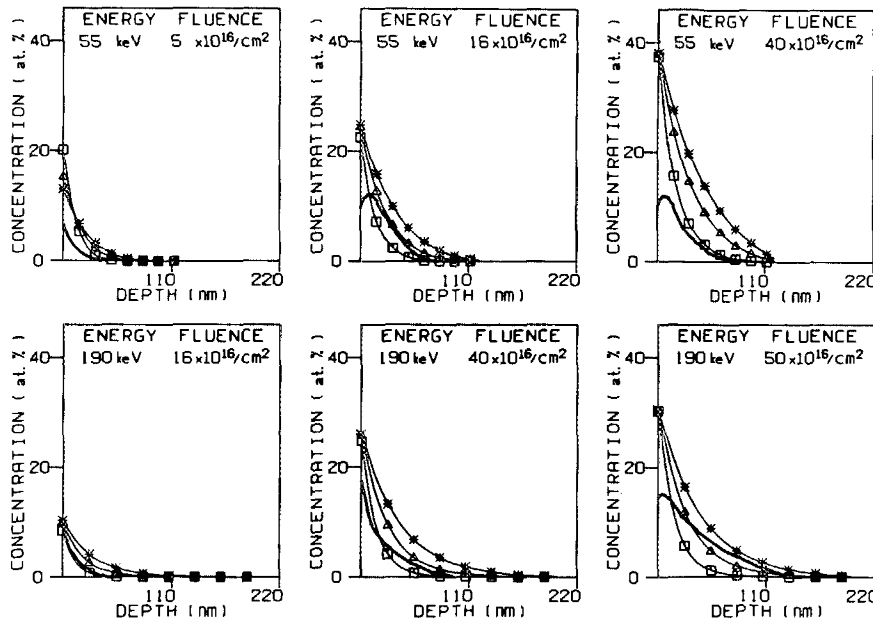

FIG. 5. Experimental (heavy line) and calculated C profiles for several values of D_C [(□: 3; △: 6; *: 10($\times 10^{-15}$ cm^2/s)], with $S = 2$ and without saturation of C at surface.

for the high fluences. As an order of magnitude estimate it may be concluded that the value of the effective diffusivity of carbon is around $D_C = 6\times 10^{-15}$ cm^2/sec.

DISCUSSION

Composition-versus-depth profiles calculated from the coupled diffusion equations (1a) and (1b) were found to be in good agreement with the experimentally determined profiles for high fluences of Ti implanted into steel. To achieve agreement the computational method had to take into account the effects of sputtering and lattice dilation, as done by previous investigators, as well as diffusion-like processes. Lattice dilation and the sputter erosion of the surface had to be included in order to obtain reasonable agreement with experiment based on the values for range and straggling given by LSS theory. Other phenomena may also be present in high fluence ion implantation, namely preferential sputtering and radiation-induced segregation. However, the agreement obtained in the present work suggests that these effects are not very significant for Ti implanted into steel. For other cases where the implanted and target species have very different atomic masses, preferential sputtering may be very significant and should be included in the calculations. Calculations including preferential sputtering are being reported in a separate paper.

The calculated curves in Figs. 2–4 show the effects of diffusivity on the Ti profiles as they evolve towards steady state at highest fluences. Atoms diffuse away from peak concentrations thereby reducing the peak maximum value and broadening the profile. This broadening, in turn, modifies the surface concentrations and retained doses of implanted

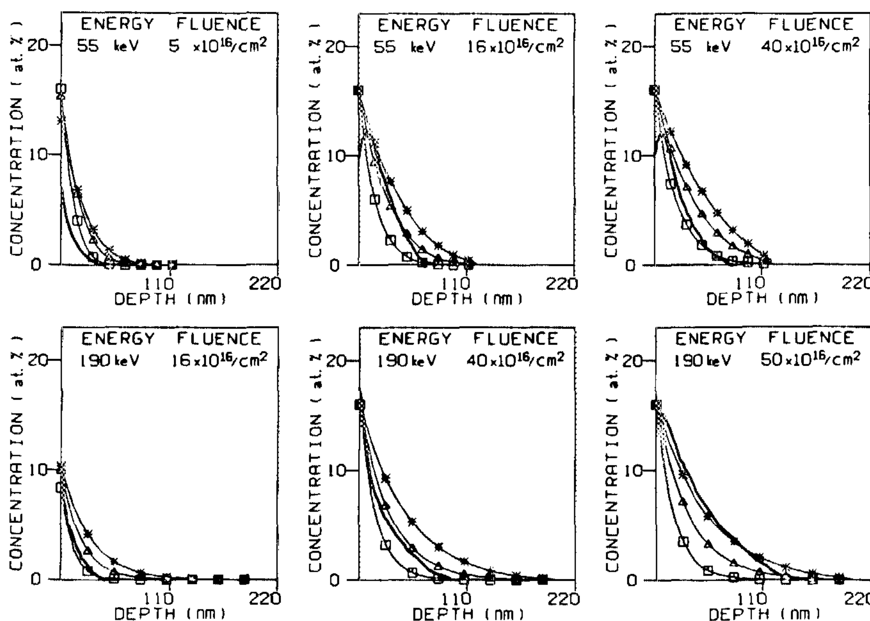

FIG. 6. Experimental (heavy line) and calculated C profiles for several values of D_C [□: 3; △: 6; *: 10($\times 10^{-15}$ cm^2/s)], with $S = 2$ and with saturation of C at surface.

[This article is copyrighted as indicated in the article. Reuse of AIP content is subject to the terms at: http://scitation.aip.org/termsconditions. Downloaded to] IP: 128.173.126.47 On: Wed, 06 May 2015 20:53:19

Ti, relative to the nondiffusing profiles. At low fluences, sputtering brings more of the out-diffusing Ti atoms to the surface, reducing the retained dose (slightly) but increasing the surface Ti concentration $[\mathrm{Ti}]^s$. This early gain of $[\mathrm{Ti}]^s$ is soon lost at higher fluences as the initial peak depth approaches the surface with its peak concentration diminished by diffusion. A steady-state profile, which would be reached short time later without diffusion, is delayed by the reduced surface concentration. A broader steady-state profile is finally achieved at higher fluences, with a comparable increase in the dose of retained Ti.

Several conclusions about the Ti implantation alloying process can be drawn from the results of the present work.

First, the sputtering yield of steel by Ti atoms is approximately 2 at fluences below those needed to form a carburized surface, but less than 2 at higher fluences. For Ar and Fe ions sputtering off Fe targets, sputtering yields of 2.2 and 2.8, respectively, have been measured.[11] It is possible that the sputtering yield of Ti is lowered when it is bonded to C.[12] When carbon is present at the surface some C atoms are also sputtered. Thus the number of Ti atoms sputtered is reduced and the sputtering yield of Ti is effectively lowered. While C atoms are lost from the surface due to sputtering, they are immediately regained from the atmosphere maintaining the C concentration at the same level. More generally, it is even possible that the anomalous dips in the self-sputtering yield of reactive metals (V, Ti, Zr, Nb, Hf, Ta) presented by Almen and Bruce[13] over twenty years ago are attributable to carburization effects.

Second, the broadened profiles obtained experimentally can be accounted for by an effective diffusivity for Ti of $D_{\mathrm{Ti}} = 6\times 10^{-15}\ \mathrm{cm^2/sec}$. Since this value of thermal diffusivity would require a temperature of 580 °C (Ref. 14) the diffusivity observed in the present problem is clearly implantation induced. Radiation-enhanced diffusion is expected to produce an effective diffusivity of this order of magnitude for implantation fluxes between $1\text{–}10\times 10^{13}$ ions/sec cm^2.[15] Furthermore, if the effective diffusion coefficient is calculated on the basis of the Kinchin–Pease relation,[7] similar values are obtained.

Finally, a diffusion-like process accounts nicely for the inward migration of C into steel during Ti implantation. The assumption of a saturation value for the C adsorbed on the surface which resulted in better agreement with experiment, is reasonable as follows. The dissociative chemisorption process, believed to produce surface carbide species[3] is in competition with a molecular desorption process which reduces the surface carbide concentration. Both processes have thermal contributions and, at room temperature, the chemisorption process cannot be expected to be 100% efficient.

The present model cannot definitely identify the mechanism of the observed effective diffusion of C, $D_{\mathrm{C}} = 6\times 10^{15}$ cm^2/sec. Three processes can contribute to this effective diffusivity value. These are thermal (nonenhanced) diffusion, radiation-enhanced thermal diffusion, and cascade mixing. Thermal diffusion of C in Fe at the sample temperature (40 °C) is 10^{-16} cm^2/sec,[16] and therefore contributes only 2% of the migration process. A recent Monte Carlo-type calculation for the collision cascade effect during the carburization of Cr-implanted Cr could account for no more than 20% of the C adsorbed as observed experimentally.[17] It appears that in the present case both collision cascades and radiation-enhanced diffusion may contribute to the inward migration of C, although the latter may be more significant. The effect of the chemical affinity of C for Ti on diffusivity still needs to be explored.

CONCLUSIONS

The formalism developed permits generation of concentration-versus-depth profiles under complicated implantation conditions such as vacuum carburization during sputtering. The present calculations provide semiquantitative evaluation of several of the dynamic processes present in high fluence reactive ion implantation. For the case of Ti implanted into 52100 steel the following can be concluded: the sputtering yield decreases from a value greater than 2 to a value smaller than 2 as fluence increases, possibly due to the incorporation of carbon with increasing fluence.

It is necessary to incorporate lattice dilation and a diffusion process for Ti in order to order to explain the experimental results; otherwise a range and straggling that are very different from those predicted by LSS theory would be required. The order of magnitude of this diffusion process is characterized by a value of $D_{\mathrm{Ti}} = 6\times 10^{-15}\ \mathrm{cm^2/sec}$, which is consistent with a cascade mixing mechanism.

The diffusion process responsible for C penetration can be described by Fick's law and is characterized by an apparent diffusion coefficient of $D_{\mathrm{C}} = 6\times 10^{-15}\ \mathrm{cm^2/sec}$. It is likely that both radiation-enhanced diffusion and cascade mixing contribute to the inward migration of C. The amount of C adsorbed at the surface can be adequately described by a one-to-one relation with the amount of Ti at the surface up to a certain saturation limit around 16 at. % carbon.

APPENDIX

Method of solution of the differential equations

The Cranck–Nicholson method can be used to solve partial differential equations coupled by boundary conditions as follows. The derivatives are replaced by difference equations:

$$\frac{\partial c}{\partial t} = (c_{i,n+1} - c_{i,n})/\Delta t,$$

$$\frac{\partial^2 c}{\partial x^2} = (1/2\Delta x^2)\,(c_{i+1,n+1} - 2c_{i,n+1} + c_{i-1,n+1} + c_{i+1,n} - 2c_{i,n} + c_{i-1,n}),$$

where c indicates concentration, and Δx and Δt are the space and time increments. The subscripts i and n denote space and time, respectively, defining a space-time grid. The two sets of equations for C and Ti, coupled by the boundary condition that links the surface concentration of carbon to that of titanium, are then converted to one system of linear equations:

$$(D)_n = (A)(X)_n,$$

$$(X)_n = ([\mathrm{C}]_{i,n}, [\mathrm{Ti}]_{i,n})$$

$$(D)_n = (d^1_{i,n}, d^2_{i,n}),$$

[This article is copyrighted as indicated in the article. Reuse of AIP content is subject to the terms at: http://scitation.aip.org/termsconditions. Downloaded to] IP: 128.173.126.47 On: Wed, 06 May 2015 20:53:19

$$d_{i,n}^1 = (D_C\Delta t/\Delta x^2)(2[\mathrm{C}]_{i,n} - [\mathrm{C}]_{i+1,n} - [\mathrm{C}]_{i-1,n}) - [\mathrm{C}]_{i,n},$$

$$d_{i,n}^2 = (D_{Ti}\Delta t/\Delta x^2)(2[\mathrm{Ti}]_{i,n} - [\mathrm{Ti}]_{i+1,n} - [\mathrm{Ti}]_{i-1,n}) - [\mathrm{Ti}]_{i,n},$$

where [C], [Ti] denote the concentrations of carbon and titanium, respectively. D_C and D_{Ti} are the apparent diffusivities of carbon and titanium, respectively. A is a bitridiagonal matrix:

$$A = \begin{bmatrix} b & c & 0 & \cdot & \cdot & \cdot \\ a & b & c & 0 & \cdot & \cdot \\ 0 & a & b & c & \cdot & \cdot \\ 0 & 0 & a & b & \cdot & \cdot \\ 0 & 0 & 0 & a & \cdot & \cdot \\ \cdot & \cdot & \cdot & \cdot & \cdot & \cdot \end{bmatrix},$$

$$a = c = \begin{bmatrix} \dfrac{D_C\Delta t}{2\Delta x^2} & 0 \\ 0 & \dfrac{D_{Ti}\Delta t}{2\Delta x^2} \end{bmatrix},$$

$$b = \begin{bmatrix} \dfrac{-D_C\Delta t}{\Delta x^2} - 1 & 0 \\ 0 & \dfrac{-D_{Ti}\Delta t}{\Delta x^2} - 1 \end{bmatrix}.$$

The matrix A can be inverted with standard subroutines. The concentrations at time step $n+1$ can be obtained from the concentrations at step n as

$$(X)_{n+1} = (A)^{-1}(D)_n.$$

[1] I. L. Singer, C. A. Carosella, and J. R. Reed, Nucl. Instrum. Methods **182/183**, 923 (1981).

[2] I. L. Singer and T. M. Barlak, Appl. Phys. Lett. **43**, 457 (1983).

[3] I. L. Singer, J. Vac. Sci. Technol. A **1**, 419 (1983).

[4] F. Schulz and K. Wittmaak, Radiat. Eff. **29**, 31 (1976).

[5] H. Krautle, Nucl. Instrum. Methods **134**, 167 (1976).

[6] J. Cranck, *The Mathematics of Diffusion*, 2nd ed., (Clarendon, Oxford, 1975), p. 4.

[7] S. M. Myers, Nucl. Instrum. Methods **168**, 265 (1980).

[8] A. H. Eltoukhy and J. E. Greene, J. Appl. Phys. **51**, 4444 (1980).

[9] A. R. Mitchell, *Computational Methods in Partial Differential Equations* (Wiley, New York, 1976), Chap. 2.

[10] I. Manning and G. P. Mueller, Comp. Phys. Commun. 7, 84 (1974).

[11] H. H. Andersen and H. L. Bay, in *Sputtering by Particle Bombardment I*, edited by R. Behrisch (Springer, Berlin, 1981), p. 173.

[12] P. Varga and E. Taglauer, J. Nucl. Mater. **111/112**, 726 (1981).

[13] O. Almen and G. Bruce, Nucl. Instrum. Methods **11**, 257 (1961).

[14] J. H. Swisher, Trans. AIME **242**, 2433 (1968).

[15] G. Dearnaley, J. H. Freeman, R. S. Nelson, and J. Stephen, *Ion Implantation*, (North-Holland, Amsterdam, 1973), p. 228.

[16] C. J. Smithells, *Metals Reference Book*, 3rd edition (Butterworths, Washington, 1962), p. 594.

[17] R. H. Bassel, K. S. Grabowski, M. Rosen, M. L. Roush, and F. Davarya, Nucl. Instrum. Methods (to be published).

[This article is copyrighted as indicated in the article. Reuse of AIP content is subject to the terms at: http://scitation.aip.org/termsconditions. Downloaded to] IP: 128.173.126.47 On: Wed, 06 May 2015 20:53:19